

# Microelectromechanical Filters for Signal Processing

Liwei Lin, Roger T. Howe, *Fellow, IEEE*, and Albert P. Pisano

**Abstract**— Microelectromechanical filters based on coupled lateral microresonators are demonstrated. This new class of microelectromechanical systems (MEMS) has potential signal-processing applications for filters which require narrow bandwidth (high  $Q$ ), good signal-to-noise ratio, and stable temperature and aging characteristics. Microfilters presented in this paper are made by surface-micromachining technologies and tested by using an off-chip modulation technique. The frequency range of these filters is from approximately 5 kHz to on the order of 1 MHz for polysilicon microstructures with suspension beams having a 2- $\mu$ m-square cross section. A series-coupled resonator pair, designed for operation at atmospheric pressure, has a measured center frequency of 18.7 kHz and a pass bandwidth of 1.2 kHz. A planar hermetic sealing process has been developed to enable high-quality factors for these mechanical filters and make possible wafer-level vacuum encapsulations. This process uses a low-stress silicon nitride shell for vacuum sealing, and experimental results show that a measured quality factor of 2200 for comb-shape microresonators can be achieved. [265]

**Index Terms**— Coupling springs, microelectromechanical filters, resonators, vacuum encapsulation.

## I. INTRODUCTION

THE USE OF electromechanical filters for signal processing dates to the 1940's. In early filters, steel plates were used as the resonators, and wires were used as the mechanical coupling elements [1]. Mechanical filters were refined between 1950–1970 into effective signal processing components and were designed into a variety of applications [2], [3].

Mechanical filters have been used where narrow bandwidth, low loss, and good stability are required. They typically have high-quality factors ( $Q$ ) combined with excellent aging characteristics. In present-day mechanical filters, nickel-iron alloys are used in constructing the resonant elements, which are capable of quality factors ranging from 10 000 to 25 000 [4]. Piezoelectric crystals, such as those commonly used in oscillators, are also sometimes used in mechanical filters.

Mechanical filters have been displaced in audio-frequency applications by the advent of integrated switched-capacitor filters, which are implemented in MOS technologies [5]. In addition, integrated analog-to-digital and digital-to-analog converters have made digital filtering attractive in some applications. Where their special properties were not essential,

mechanical filters were noncompetitive because of higher manufacturing cost and larger size (typically, cylinders several centimeters in length and approximately 1 cm in diameter). With the advent of CMOS very large-scale integration (VLSI) technology, it became feasible to integrate switched-capacitor filters with other functional blocks to fabricate single-chip microsystems (e.g., in a one-chip modem).

If a filter using micromechanical elements could be fabricated by integrated circuit (IC) processes, then many of their technological drawbacks would be eliminated. In particular, micromechanical filters could emerge as functional blocks in integrated microsystems. Somewhat similar motivations were behind efforts at the Westinghouse Research and Development Center in the 1960's to develop micromechanical resonant structures for filtering and other applications [6]. The pioneering "resonant gate transistor" was a field-effect transistor with a vibrating metal beam replacing the gate. The beam was resonated vertical to the substrate using electrostatic forces applied by an underlying electrode. Typical dimensions of the metal thin-film beams were 0.1 mm long and 5–10  $\mu$ m thick. Typical quality factors were 500 at 5 kHz. The project was abandoned due to low  $Q$ 's, high-temperature coefficients of the resonant frequency, and aging of the metal films. In addition, the nonlinear electrostatic drive would impose severe constraints on the amplitude of the input signal and, thus, the dynamic range of the filter.

The advances in micromachining processes and in microresonator materials and design [7], [8] have opened the feasibility of integrated micromechanical filters. Microresonators fabricated from polycrystalline silicon (a low-loss material), driven by interdigitated electrodes (which provide a linear excitation), and suspended by folded flexures (for a linear spring-rate to very large displacements) are very attractive as building blocks for mechanical filters. In addition, laterally driven structures benefit from having all critical features defined in one masking level, which enables the designer to implement such features as differential drive and split combs for levitation suppression without the need for process changes [9]. To be generally useful, these micromechanical structures must be integrated together with associated microelectronic interface circuits. Several processes have already demonstrated the capability of integration of circuitry and moving polysilicon microstructures [10], [11].

The operation of comb-drive microstructures in the ambient atmosphere results in low-quality factors of less than 100 due to air damping [12] above and below the moving microstructure. Resonance quality factors from 100 to 10 000 are required for these filters for practical applications, hence, the hermetic sealing process has to be established. Previously, several

Manuscript received April 16, 1997; revised December 20, 1997. This work was supported by the Berkeley Sensor and Actuator Center, an NSF/Industry/University Cooperative Research Center. Subject Editor, D. Cho.

L. Lin is with the Department of Mechanical Engineering and Applied Mechanics, University of Michigan, Ann Arbor, MI 48109-2125 USA.

R. T. Howe is with the Department of Electrical Engineering and Computer Science, University of California, Berkeley, CA 94720 USA.

A. P. Pisano is with the Department of Mechanical Engineering, University of California, Berkeley, CA 94720 USA.

Publisher Item Identifier S 1057-7157(98)06343-4.

processes for the vacuum sealing of narrow microbridges have been demonstrated, and these have used epitaxial silicon [13], [14], polysilicon [15], [16], and silicon-rich silicon nitride [17] as microshell materials. However, the vacuum sealing of microfilters based on comb-drive structures encounters difficulty due to the large area and relatively soft suspensions of the microresonators.

This paper presents design techniques, microstructural layouts, and test results of series microelectromechanical filters based on mechanically coupled polysilicon comb microresonators. A wafer-level vacuum sealing process is introduced to demonstrate the feasibility of an integrated vacuum packaging procedure. These approaches show promise for achieving high signal-to-noise ratio (with on-chip detection circuits) and high-quality factors of microelectromechanical filters. In conclusion, the techniques and research directions on materials, vacuum encapsulation, and manufacturing procedures are discussed.

## II. FILTER TOPOLOGIES AND THEORETICAL MODELING

### A. Series Micromechanical Filters

The principle of a series mechanical filter is illustrated in Fig. 1, which shows springs  $k_{ij}$  linking two adjacent resonators having masses  $M_i$  and  $M_j$  and springs  $k_i$  and  $k_j$ . In contrast to the frequency response of the uncoupled single resonators, the filter in Fig. 1 can be configured to have an improved bandpass characteristic by proper selection of resonators, coupling springs, and bridging springs which link nonadjacent resonators (note that bridging springs have not been drawn in Fig. 1). Hence, higher order systems with multiple-coupling springs enable synthesis of high-quality bandpass filters. Signals, in the form of current or voltage, are converted by an input electromechanical transducer into mechanical vibrations at the filter, pass through the series filter, and are then converted back into electrical signals by an output electromechanical transducer. For example, magnetostrictive and piezoelectric transducers are commonly used in conventional mechanical filters [4].

The series filter concept has been implemented by using coupled electrostatically driven polysilicon resonant structures. Fig. 2 shows the design layout of a series two-resonator filter, with a square-truss coupling spring [18]. The input and output electrostatic combs function as linear electromechanical transducers as long as they are biased at a dc voltage which is much larger than the amplitude of the signal voltage [7]. High-order micromechanical filters can be realized by adding more microresonators with coupling springs [19] and bridging springs [20].

An electromechanical filter may also be realized by combining the current outputs of two (or more) microresonators with resonance frequencies which differ by a specific designed amount. The outputs of the single microresonators are then combined with appropriate control of the phase of microresonator motional currents. Either a bandpass filter or a notch filter can be realized [21]. For the case of the bandpass filter, the relative phase difference between microresonators is selected such that currents combine in the interval between

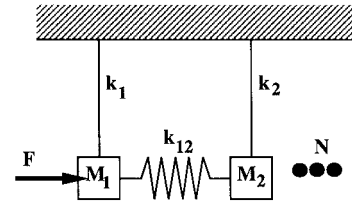


Fig. 1. Conceptual diagram of a coupled-series N-resonator filter.

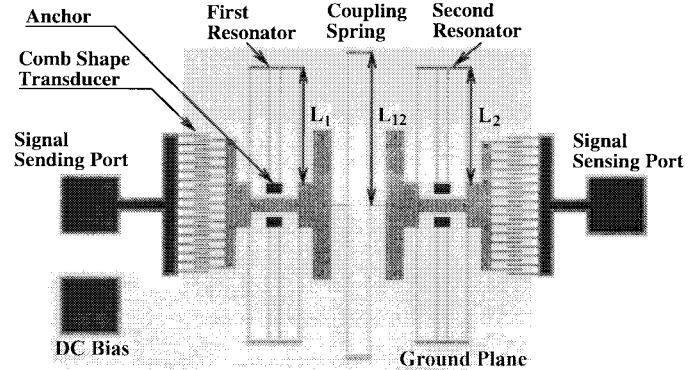


Fig. 2. Layout of a series two-resonator mechanical filter.

the two resonances (currents are in phase), but subtract outside this interval (currents are approximately  $180^\circ$  out of phase).

### B. Mechanical Model

An N-resonator series filter with only nearest neighbor coupling springs can be modeled mechanically as shown in Fig. 3. The transfer function of the output displacement  $X_n$  to the input force  $F$  is essential since the derivative of the output displacement is proportional to the sense current [7]. The transfer function can be expressed as

$$\frac{X_n}{F} = \frac{1}{G_{2n}S^{2n} + G_{2n-1}S^{2n-1} + G_{2n-2}S^{2n-2} + \dots + G_0} \quad (1)$$

where  $G_{2n}$  and  $G_{2n-1} \dots G_0$  are constants in the transfer function and can be designed by changing the filter geometry. The equivalent mass, spring rate, and damping coefficient for the individual resonators are given by [7]

$$M_i = M_{ip} + 0.3714M_{ib} \quad (2)$$

$$k_i = 2E_p h \left( \frac{w_i}{L_i} \right)^3 \quad (3)$$

$$D_i = (M_i k_i)^{1/2} Q_i \quad (4)$$

where  $M_{ip}$  and  $M_{ib}$  represent the mass of the plate and the mass of the folded beams of the  $i$ th resonator and  $w_i$  and  $L_i$  are the width and length of the eight struts in its folded suspension. The thickness of the microstructure is  $h$ , and the Young's modulus of polysilicon is  $E_p$ . The damping coefficient is determined experimentally from the measured quality factor  $Q_i$  although reasonable models based on viscous drag have been developed [7], [12], [22]. Quality factors ranging from less than 100 at atmospheric pressure in air to approximately 50000 in high vacuum [8] have been measured.

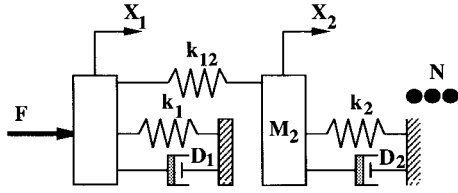


Fig. 3. Mechanical model of a series N-resonator filter.

The interresonator coupling spring stiffnesses are given by

$$k_{ij} = E_p h \left( \frac{w_{ij}}{L_{ij}} \right)^3 \quad (5)$$

in which  $w_{ij}$  and  $L_{ij}$  are the width and length of the square-truss coupling spring as illustrated in Fig. 2.

From an electronic system design standpoint, the transfer function relating input voltage to output current  $I_o/V_i$  is most useful. Such a relation may be obtained by relating the internal mechanical parameters  $F$  and  $X_n$  to the corresponding electrical input and output through the phasor relations

$$F = V_{P_i} \left( \frac{\partial C}{\partial x} \right)_i V_i \quad (6)$$

$$I_o = V_{P_o} \left( \frac{\partial C}{\partial x} \right)_o j\omega X_n \quad (7)$$

where  $V_{P_i}$  and  $V_{P_o}$  represent the dc bias at the drive (input) and sense (output) ports, respectively, and  $(\partial C/\partial x)_i$  and  $(\partial C/\partial x)_o$  are the capacitive changes with respect to comb motion at the respective ports. For the particular case of comb-driven transducers, the value  $\partial C/\partial x$  is a constant and can be theoretically approximated (and underestimated since fringing fields are neglected) [23] as

$$\frac{\partial C}{\partial x} = \frac{2N\epsilon_0 h}{d_f} \quad (8)$$

where  $N$  is the number of the comb fingers,  $\epsilon_0$  is the permittivity, and  $d_f$  is the gap between the fingers. Hence, the filter transconductance can be expressed in phasor form as (9), given at the bottom of the page.

### C. Electrical Model

Most previous analyses for filters in the macroscale use the analogy modeling method to transform mechanical elements into equivalent electrical elements in order to apply the large body of electrical filter design tools. The theoretical transformation parameter  $\eta$  (shown in Fig. 4 for a comb-shaped transducer) can be theoretically obtained by first deriving the equivalent resistance, inductance, and capacitance (RLC) circuit elements for a single comb-driven resonator and then generalizing the resulting  $\eta$  for the case of a complete filter.

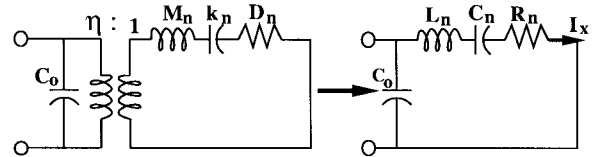


Fig. 4. The equivalent circuit for a comb-shaped transducer.

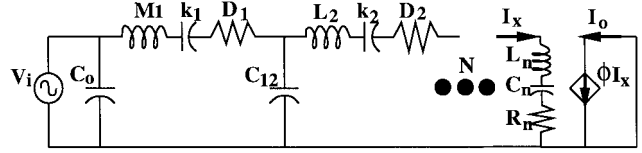


Fig. 5. Equivalent circuit for a series N-resonator filter.

From the above, one finds

$$\eta = \frac{1}{V_{P_i} \left( \frac{\partial C}{\partial x} \right)_i} \quad (10)$$

From the theory of indirect analogy, force and velocity in a mechanical system can be treated as voltage and current in an electrical system. Hence, the electrical equivalent circuit for the series N-resonator filter in Fig. 3 can be further illustrated in Fig. 5 for a purely electrical model including two transducers. ( $C_0$  is the dc capacitance of the comb fingers.) The electrical elements are related to the mechanical elements as follows:

$$L_i = M_i \eta^2 \quad (11)$$

$$C_i = \frac{1}{k_i \eta^2} \quad (12)$$

$$R_i = D_i \eta^2 \quad (13)$$

$$C_{ij} = \frac{1}{k_{ij} \eta^2} \quad (14)$$

The theoretical form of  $I_x$  (as defined in Fig. 5) can be derived by pure electrical analysis, and the amplification factor  $\phi_i$  in Fig. 5 can be expressed as

$$\phi_i = \frac{I_o}{I_x} = \frac{V_{P_o} \left( \frac{\partial C}{\partial x} \right)_o}{V_{P_i} \left( \frac{\partial C}{\partial x} \right)_i} \quad (15)$$

The final form of  $I_o/V_i$  is exactly the same as (9).

## III. FABRICATION AND MEASUREMENTS

### A. Fabrication Processes

These filters have been fabricated via the polysilicon surface-micromachining process previously used for lateral

$$\frac{I_o}{V_i} = \frac{j\omega V_{P_i} V_{P_o} \left( \frac{\partial C}{\partial x} \right)_i \left( \frac{\partial C}{\partial x} \right)_o}{G_{2n}(j\omega)^{2n} + G_{2n-1}(j\omega)^{2n-1} + G_{2n-2}(j\omega)^{2n-2} + \dots + G_0} \quad (9)$$

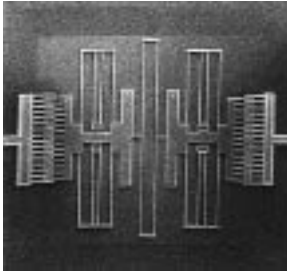


Fig. 6. The SEM photo of a series two-resonator filter.

TABLE I  
DIMENSIONS OF TESTED SERIES MICROFILTERS

dimensions	Design	Measured
Number of resonators	2	2
Beam length(resonator 1)[ $\mu\text{m}$ ]	150	150
Beam length(resonator 2)[ $\mu\text{m}$ ]	150	150
Beam width[ $\mu\text{m}$ ]	2	1.7
Thickness [ $\mu\text{m}$ ]	2	1.8
Coupling spring length[ $\mu\text{m}$ ]	150	150
Coupling spring width[ $\mu\text{m}$ ]	1	0.8

resonators [7], [8], with a polysilicon thickness of approximately  $2 \mu\text{m}$ . The folded suspensions are  $2 \mu\text{m}$  wide, whereas the more compliant coupling springs are only  $1 \mu\text{m}$  wide. All key structures such as the comb, folded-beam resonators, and coupling springs have been defined and etched in a single masking step. A low-pressure chemical-vapor deposition (LPCVD) oxide nonerodible etch mask has been used to achieve nearly vertical polysilicon sidewalls. A scanning electron micrograph (SEM) of a two-resonator series filters is shown in Fig. 6.

**B. Measurements**

The electrical responses of the fabricated prototype filters have been measured using an off-chip modulation-sensing technique in air [8], [23]. Table I shows the designed and measured dimensions of the series two-resonator filter. Fig. 8 shows the spectrum response of a two-resonator series microfilter (with a coupling spring length of  $150 \mu\text{m}$ ) and the theoretical (downward triangular symbols) result. The design of the mechanical spring can change the characteristics of the spectrum. A stiffer coupling spring with a length of  $100 \mu\text{m}$  can produce a wider bandwidth, but also increase the passband ripple, and a notch filter may be realized [24]. On the other hand, the spectra of a single resonator has been measured to determine several parameters such as Young’s modulus and a quality factor as shown in Fig. 7. The Young’s modulus is estimated to be about 150 GPa, and the quality factor is about 30. Table II is the summarized characteristics of the spectra showing in Fig. 8 which shows remarked improvement over that for a single microresonator.

**IV. INTEGRATED VACUUM-ENCAPSULATION PROCESS**

In order to increase the quality factor of these microfilters for practical application, vacuum packages are required. A wafer-level integrated vacuum-encapsulation process is attrac-

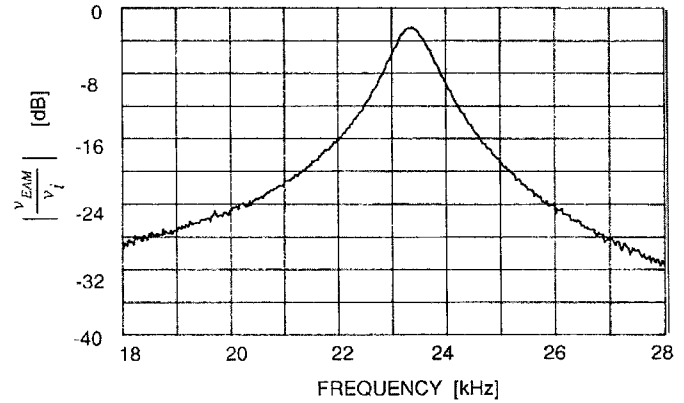


Fig. 7. Experimental measurement of a single-comb resonator operated in air.

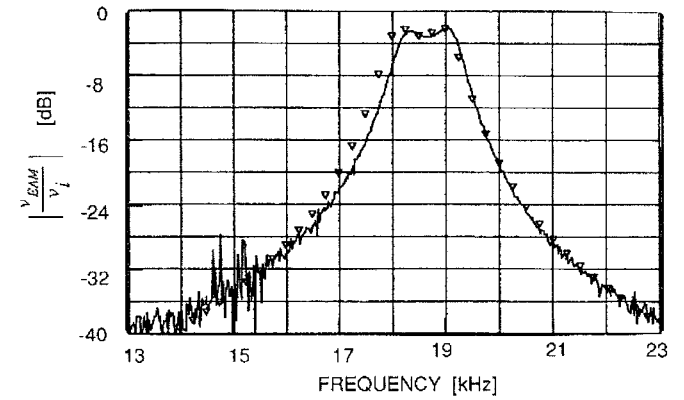


Fig. 8. Experimental and theoretical results of the series two-resonator micromechanical filter.

TABLE II  
CHARACTERISTICS OF TESTED SERIES MICROMECHANICAL FILTERS

Characteristics	Series Filter
Center frequency ( $f_0$ ) [KHz]	18.7
3dB bandwidth ( $BW_3$ ) [KHz]	1.2
20dB bandwidth( $BW_{20}$ ) [KHz]	3.2
Fractional bandwidth ( $\frac{BW_3}{f_0}$ )	6.4%
Passband ripple [dB]	1.5
Shape factor ( $\frac{BW_{20}}{BW_3}$ )	2.7
Quality factor ( $\frac{f_0}{BW_3}$ )	15.6

tive since expensive postpackaging may be avoided. LPCVD silicon-rich silicon nitride has been used to vacuum encapsulate these comb-shape microstructures with a large area and soft suspensions.

**A. Layout and Fabrication Process**

The actual (in scale) layout for the vacuum-encapsulation process is illustrated in Fig. 9, where the comb-drive microstructure is covered by a microshell. The microshell is drawn in transparent such that both the comb resonator and ground plane can be clearly seen. The comb structure has eight suspended struts which are  $150 \mu\text{m}$  long and  $2 \mu\text{m}$  wide. Both the thick and thin phosphorus-doped LPCVD  $\text{SiO}_2$  (PSG) layers cover the whole comb structure. The thick PSG layer extends at least  $25 \mu\text{m}$  away from the edges of the comb resonator. The thin PSG layer extends another  $5 \mu\text{m}$

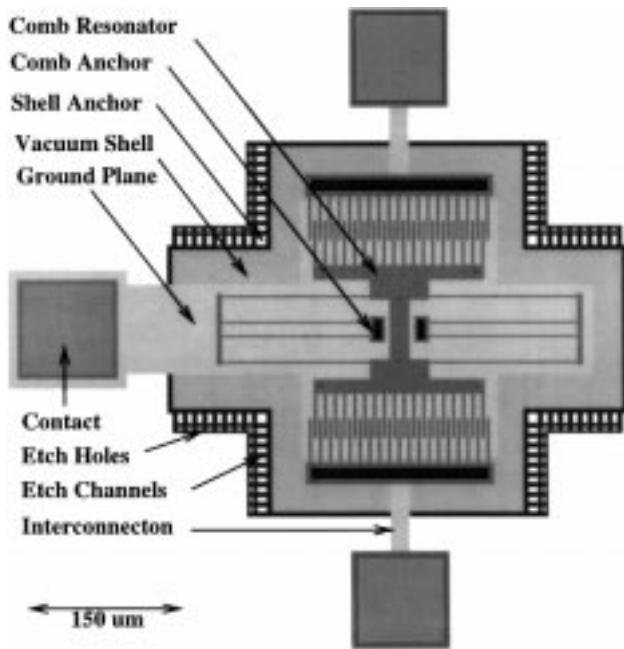


Fig. 9. Design layout of a vacuum-encapsulated lateral microresonator.

more away from the thick PSG layer. These extensions are to ensure that safe margins are established during the wet PSG etching process. The etch channels are represented by the gray rectangles around the microshell and will be subsequently filled by low-stress nitride during the sealing process. Those large white rectangles which are right next to etch channels are the landing anchors of the shell. Finally, the light grey squares are etch holes which are  $5 \mu\text{m}$  in width.

Fig. 10 illustrates the process sequence. Standard surface-micromachining steps which have been used to fabricate the microelectromechanical filters are carried out through the second polysilicon patterning in four masks as shown in Fig. 10(a). Without etching away the sacrificial PSG (phosphorus-doped LPCVD  $\text{SiO}_2$ ),  $7 \mu\text{m}$  of additional PSG is deposited to cover the microstructure. This thick PSG layer is deposited using two sequential depositions and densifications to reduce the nonplanar topology. After the vacuum shell area (Mask #5) is patterned, 5:1 BHF (buffered HF) is used to define the microshell area as illustrated in Fig. 10(b). A  $1\text{-}\mu\text{m}$ -thick PSG is deposited, patterned, and etched in 5:1 BHF to form etch channels (Mask #6) as shown in Fig. 10(c). A  $1\text{-}\mu\text{m}$ -thick LPCVD low-stress nitride is then deposited, and etch holes are defined (Mask #7) and etched in a plasma etcher [Fig. 10(d)]. All PSG inside the shell is then etched away in concentrated HF. After rinsing in water and methanol, the wafer is dried using the supercritical  $\text{CO}_2$  process [25]. A yield of over 90% freestanding comb-shape resonators is achieved in the initial tests. Finally, a  $2\text{-}\mu\text{m}$ -thick LPCVD low-stress nitride layer is deposited at a deposition pressure of 300 mTorr to seal the shell, and contact pads are opened (Mask #8) as shown in Fig. 10(e).

### B. Fabrication Results

Fig. 11 is the SEM microphoto of a vacuum-sealed lateral microresonator, with beams  $150 \mu\text{m}$  long and  $2 \mu\text{m}$  wide. A

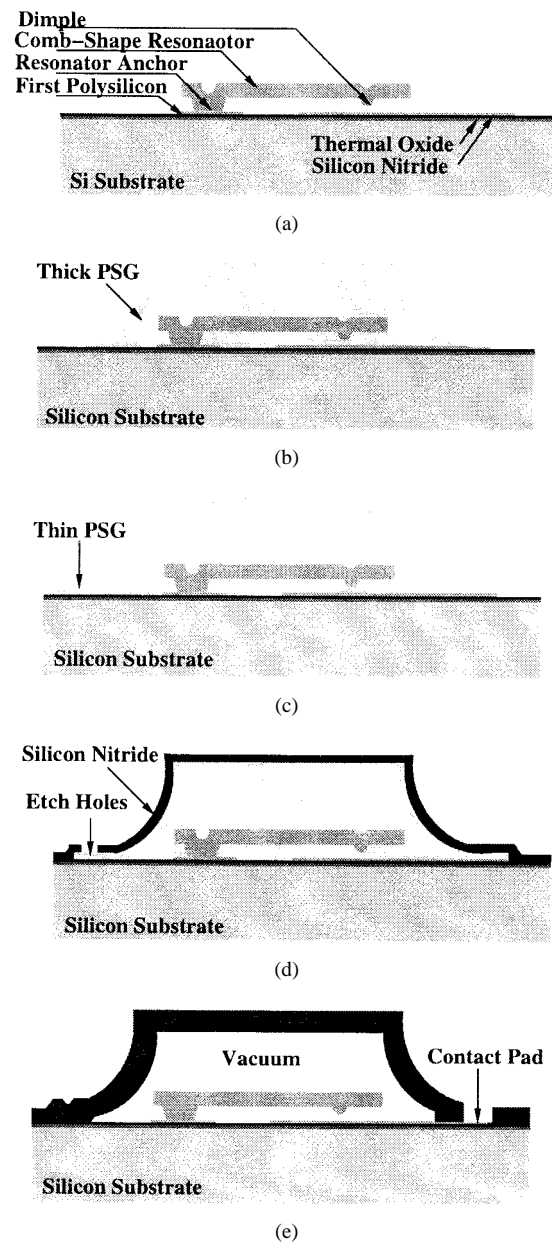


Fig. 10. Process flow for the vacuum-encapsulated microresonators.

contact pad is shown with the covering nitride layer removed. The nitride shell has a height of about  $12 \mu\text{m}$  as seen standing above the substrate. There are microbubbles in the surface of the nitride shell which are created during the thick PSG deposition process [26]. It is suspected that these microbubbles are also produced by residual polystringers.

Fig. 12 is an SEM micrograph of a cleaved wafer showing a cross section of a resonator in the microshell. It was observed that the surface of the resonator has a uniform light blue color on both sides (top and bottom). This color indicates that the nitride-forming gas (dichlorosilane and ammonia) diffused into the nitride shell through the etch channels. Fig. 13 is a micrograph showing a magnified cross section of the broken comb finger in Fig. 12. It can be identified in Fig. 13 that a layer of nitride of about 1500 Å has covered the polysilicon. Different colors from light yellow to light blue with good

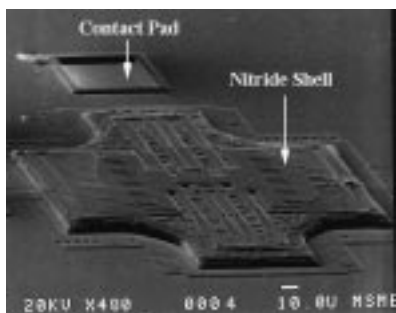


Fig. 11. An SEM microphoto of a vacuum-encapsulated lateral microresonator.

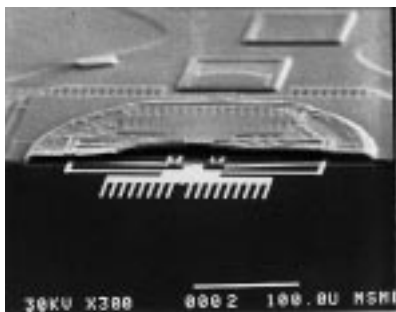


Fig. 12. Shell and freestanding comb structure cross section as seen in an SEM.

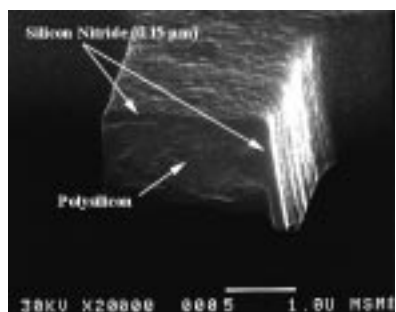


Fig. 13. A close view of the broken tooth showing a thin nitride layer deposited on the microstructure inside the shell.

uniformity have been observed in different designs of shells. Similar effects have been reported in surface-micromachined flow channels [27].

### C. Experiments

These vacuum-encapsulated lateral microresonators have been observed in operation under an optical microscope. An off-chip measurements scheme [23] is used to measure frequency spectrums of microresonators both in air and in encapsulation. It is found that an unencapsulated resonator resonating at 17 kHz will subsequently resonate at 24 kHz after going through the vacuum-encapsulation process. The uniform deposition of excess nitride over the resonator structure is probably the primary cause. The microresonator can be successfully operated with only a 5-V dc bias and 0.3-V ac signal. This result could not be achieved previously in air.

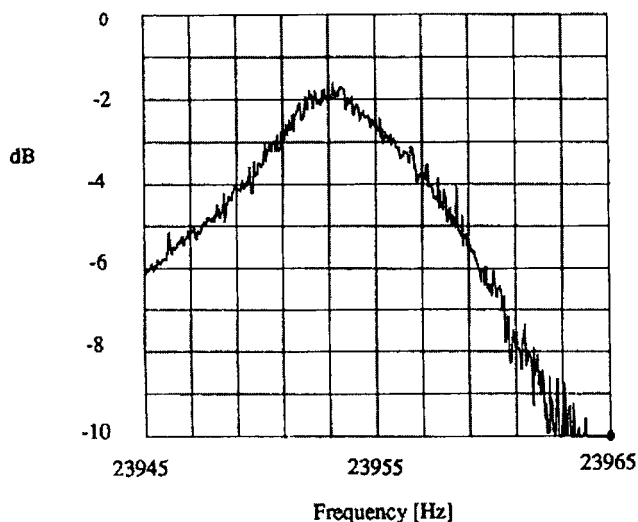


Fig. 14. Experimental measurement of a vacuum-encapsulated lateral microresonator.

Fig. 14 is a spectrum measurement of a vacuum-encapsulated lateral microresonator. The center frequency is 23 953 Hz, and the quality factor is 2200. Reports have shown that quality factor of these comb resonator is less than 100 when operated in air while it can reach 50 000 when operated in high vacuum ( $10^{-7}$  Torr) [8]. The quality factor of 2200 corresponds to a pressure of about 200–300 mTorr [28] inside the shell. Since the deposition pressure of the sealing process is 300 mTorr, part of the gas inside the shell is presumed to have continued reacting and is consumed during the process.

This residual pressure inside the microshell could be reduced if LPCVD polysilicon is used as the shell material. The source gas for polysilicon deposition can continue reacting and a high vacuum can be achieved [15]. Moreover, the polysilicon shell can provide an electrical shield and provide electrical protection as well as mechanical protection to the sealed structures. However, an additional insulation material such as silicon nitride should be added between the noninsulator and the electrical feedthroughs. Some reports suggested that permeable polysilicon actually allows concentrated HF to penetrate and etch away the PSG layer underneath [29], [28]. This etching mechanism could save one–two masks from the current shell process [30]. The high-temperature drive-in process in the standard microstructure fabrication could be modified by low-temperature as-deposited LPCVD polysilicon with a subsequent suitable rapid thermal annealing (RTA) annealing for stress relief [21] such that the whole shell process would be fully compatible with postintegrated circuit processes.

### V. DISCUSSIONS

The results of microelectromechanical filters operating in air and the successful demonstration of the wafer-level vacuum-encapsulation process indicate that microelectromechanical filters are a promising direction for high- $Q$  narrow-band signal processing applications. Table III lists the comparisons between micro and macromechanical filters, and it is clear that

TABLE III  
COMPARISONS BETWEEN MACRO AND MICROMECHANICAL FILTERS

	Macro	Micro
Percent Bandwidth	2% to 10%	6%(in air)
Temperature coefficient	60 ppm/°C	10 ppm/°C
Aging(Ten years)	750 ppm	??
Compatibility with IC	No	Yes
Multifunctional Chip	No	Yes

microelectromechanical filters have great potential in terms of being built with functional blocks in a single chip as a multifunctional system. However, there are several technical issues for developing practical implementations of these filters. Prospects on the materials, vacuum encapsulation, and manufacturing issues are provided in this section.

#### A. Materials

The prototype filters are fabricated from LPCVD polycrystalline silicon, which is well known for having a process-dependent residual strain. The folded suspensions used for the prototype filters have spring rates which are nearly insensitive to the average residual strain (tensile or compressive) in the film since they are able to release stress being freed from the substrate [7], [31]. The square-truss coupling springs are attached to the resonators at their center points. Therefore, they are also free to expand or contract after removal of the sacrificial layer. A second benefit of folded suspensions is that they largely isolate the filter from strains in the substrate caused by thermal expansion or packaging. Aging should be less of a problem with microelectromechanical filters than with conventional mechanical filters since polysilicon is a high- $Q$  material.

The filter characteristics are a function of the Young's modulus and the density of polysilicon, both of which vary with temperature. For fine-grained polysilicon, the calculated temperature coefficient of Young's modulus for microcrystalline silicon is  $-75$  ppm/°C [32]. For linear microresonators with folded-beam suspensions, the temperature coefficient of the resonance frequency  $TC_f$  can be determined by differentiating with respect to temperature  $T$ , yielding an expression of the form

$$TC_f = \frac{1}{2}(TC_E + TC_h) \quad (16)$$

where  $TC_E$  and  $TC_h$  are the temperature coefficients of the Young's modulus and thermal expansion (2.5 ppm/°C) [33], respectively. Equation (16) predicts a  $TC_f$  of  $-36$  ppm/°C, which is better than that of conventional mechanical filters at 60 ppm/°C [4]. An experimental study has demonstrated that  $TC_f$  is only  $-10$  ppm/°C for *in situ* phosphorus-doped polysilicon deposited at 610°C [34]. However, the temperature coefficient of frequency of *packaged* resonators must be measured in order to make a fair comparison.

Although the initial test devices are fabricated by polysilicon, other process sequences and materials are possible and may have advantages for particular applications. For example, single-crystal silicon lateral resonant microstructures identical in design have been fabricated by means of a wafer-bonding

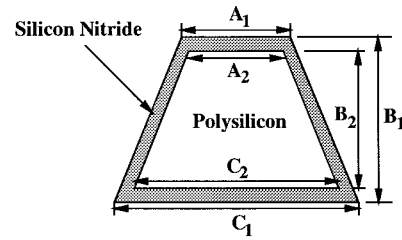


Fig. 15. A composite beam with a trapezoidal cross section.

process [35], [36]. A major advantage of the polysilicon structures is that they can be fabricated along with microelectronic functional blocks as demonstrated by the commercial microaccelerometers [38].

#### B. Vacuum Encapsulation

Quality factor determines the characteristics of the mechanical filter, and it increases as the environment pressure decreases [28]. In order to achieve high-quality factors, micromechanical filters must be packaged in a moderate-high vacuum. A vacuum ambient could be provided by a hermetic package although this approach would involve greater cost. The vacuum-encapsulation process described in this paper has demonstrated the feasibility of using the integration process to package microfilters under a thin-film vacuum cavity [39]. For the relatively small cost of a few additional deposition and masking steps, micromechanical filter chips could be fabricated with no need for special and expensive hermetically sealed packages.

A few design issues should be addressed for this integrated vacuum-encapsulation process. First, the nitride shell, which may have been statically charged [9], may cause an interesting frequency doubling effect. It has been found that with a 0-V dc bias and a 3-V ac signal, the microresonator with natural frequency of 24 kHz can resonate when excited by a 12-kHz signal. This second-order forcing-function-induced resonance has not been observed in air probably due to the heavy viscous air damping effect [40]. Furthermore, this second harmonic term is negligible while the resonator is driven in air and the dc bias voltage is much larger than the ac input.

Second, since a thin layer (1500 Å) of silicon nitride has deposited onto the surface of the resonator, the resonant frequency of the resonator is changed. The cross section of the beam is measured under SEM and illustrated in Fig. 15, where a trapezoidal cross section is the result of plasma etch. It is measured that  $A_2$  is  $1.3 \mu\text{m}$ ,  $C_2$  is  $1.85 \mu\text{m}$ , and  $B_2$  is  $2.4 \mu\text{m}$  while the nitride layer has the thickness of 1500 Å. The moment of inertia of this trapezoidal cross section coated with a second material, silicon nitride, can be represented as

$$I_{\text{tra}} = \frac{E_n}{48E_p} \left[ B_1(A_1 + C_1)(A_1^2 + C_1^2) - B_2 \left( 1 - \frac{E_p}{E_n} \right) (A_2 + C_2)(A_2^2 + C_2^2) \right] \quad (17)$$

where  $I_{\text{tra}}$  is the effective moment of inertia with respect to polysilicon and  $E_n$  and  $E_p$  are the Young's modulus of nitride and polysilicon, respectively. The resonant frequency  $f_r$  is

$$f_r = \frac{1}{2} \sqrt{\frac{24E_p I_{\text{tra}}}{(M_p + 0.3714M_b)L_{\text{beam}}^3}} \quad (18)$$

where both  $M_p$  and  $M_b$  are the mass of the plate and of the supporting beams and both include the coated thin nitride layers. Experimentally, a 17-kHz microresonator without going through the shell process has been found to resonate at 24 kHz inside the microvacuum shell. Equation (18) predicts a resonant frequency of 23.4 kHz.

Another issue to be considered is the possibility of the nitride shell collapsing under ambient pressure. Nitride shells with different designs have been tested under a surface profiler Alpha Step 200. The measured deflections are from 2 to 4  $\mu\text{m}$  at the center of the 3.5- $\mu\text{m}$ -thick nitride shells fabricated between 300–400  $\mu\text{m}$  in length. These results are qualitatively consistent with the theoretical calculations [39]. However, if a large area is to be covered by a thin nitride shell, supporting posts may be a necessary design addition.

### C. Manufacturing

Conventional mechanical filters require the manufacturing of resonators, coupling wires, and transducers, as well as bonding, and final trimming. For microelectromechanical filters, the IC batch process is used to fabricate the resonators, coupling elements, and electronic interface together, thereby achieving the advantages of batch fabrication and avoiding time-consuming steps such as the serial bonding of coupling wires to resonators. However, the IC process is not sufficiently well controlled that the microresonators can be fabricated without some means of trimming for final adjustment of the filter characteristics. In order to trim the resonant frequencies, processes for adding or removing material from the resonator must be developed. Some options for trimming are laser etching or laser-induced local deposition [41], similar processes using focused ion beams, or the laser-induced evaporation of metal films deposited on the resonator. However, these processes should be conducted before the encapsulation process. Recent development in electrical trimming by using parallel-plate capacitors seems to provide a new way for postprocess trimming [19]. If successfully developed, this method can potentially solve the controllable and repeatable problems for these microelectromechanical filters.

## VI. CONCLUSION

In conclusion, this paper has demonstrated the concept of microelectromechanical bandpass filters including the wafer-level vacuum-encapsulation process for audio-frequency applications. In addition to being a new technology for fabricating mechanical filters, there may be potential for developing functional blocks which can be used in integrated microsystems. For comb-shape microfilters with suspension beams having a 2- $\mu\text{m}$ -square cross section, the frequency range is from

approximately 5 kHz to on the order of 1 MHz. A series two-resonator bandpass microfilter has been fabricated with a measured center frequency of 18.7 kHz and a bandwidth of 1.2 kHz. A planar hermetic encapsulating process has been demonstrated by using a low-stress nitride shell. It enables high-quality factors for microelectromechanical filters, independent of the nature of the ambient environment. A vacuum-sealed microresonator has a measured quality factor of 2200 at a center frequency of 24 kHz. Higher quality factors can be achieved by using polysilicon as the sealing material.

## ACKNOWLEDGMENT

The authors would like to thank Dr. C. T.-C. Nguyen for valuable discussions and the helping in the spectrum measurements and K. McNair for valuable discussions in the vacuum-encapsulation process. The devices were fabricated in the University of California at Berkeley Microfabrication Laboratory.

## REFERENCES

- [1] R. Adler, "Compact electromechanical filters," *Electronics*, vol. 20, pp. 100–105, 1947.
- [2] J. C. Hathaway and D. F. Babcock, "Survey of mechanical filters and their applications," *Proc. IRE*, vol. 45, pp. 5–16, Jan. 1957.
- [3] R. A. Johnson, M. Borner, and M. Konno, "Mechanical filters—A review of progress," *IEEE Trans. Sonics Ultrason.*, vol. SU-18, pp. 155–170, 1971.
- [4] R. A. Johnson, *Mechanical Filters in Electronics*. New York: Wiley, 1983.
- [5] R. Gregorian and G. C. Temes, *Analog MOS Integrated Circuits for Signal Processing*. New York: Wiley, 1986.
- [6] H. C. Nathanson, W. E. Newell, R. A. Wickstrom, and J. R. Davis, "The resonant gate transistor," *IEEE Trans. Electron Devices*, vol. ED-14, pp. 117–133, 1967.
- [7] W. C. Tang, T. C. Nguyen, and R. T. Howe, "Laterally driven polysilicon resonant microstructures," *Sens. Actuators*, vol. 20, pp. 25–32, 1989.
- [8] W. C. Tang, T. C. Nguyen, M. W. Judy, and R. T. Howe, "Electrostatic-comb drive of lateral polysilicon resonators," *Sens. Actuators A-Physical*, vol. 21, pp. 328–331, 1990.
- [9] W. C. Tang, M. G. Lim, and R. T. Howe, "Electrostatic comb drive levitation and control method," *IEEE J. Microelectromech. Syst.*, vol. 1, pp. 170–178, 1992.
- [10] R. T. Howe, W. Yun, and P. R. Gray, "Surface micromachined, digitally force-balanced accelerometer with integrated CMOS detection circuitry," in *Dig. IEEE Solid-State Sensor and Actuator Workshop*, 1992, pp. 126–131.
- [11] R. T. Howe, B. E. Boser, and A. P. Pisano, "Polysilicon integrated microsystems: Technologies and applications," *Sens. Actuators*, vol. A56, pp. 167–77, 1996.
- [12] Y. H. Cho, B. M. Kwak, A. P. Pisano, and R. T. Howe, "Viscous energy dissipation in laterally oscillating planar microstructures: A theoretical and experimental study," in *Proc. IEEE Micro Electro Mechanical Systems Workshop (MEMS93)*, pp. 93–98.
- [13] K. Ikeda, H. Kuwayama, T. Kobayashi, T. Watanabe, T. Nishikawa, T. Yoshida, and K. Harada, "Silicon pressure sensor integrates resonant strain gauge on diaphragm," *Sens. Actuators*, vol. A21-A23, pp. 146–150, 1990.
- [14] ———, "Three-dimensional micromachining of silicon pressure sensor integrating resonant strain gauge on diaphragm," *Sens. Actuators*, vol. A21-A23, pp. 1007–1010, 1990.
- [15] J. J. Sniegowski, H. Guckel, and T. R. Christenson, "Performance characteristics of second generation polysilicon resonating beam force transducers," in *Tech. Dig. IEEE Solid-State Sensor and Actuator Workshop*, 1990, pp. 9–12.
- [16] H. Guckel, J. J. Sniegowski, and T. R. Christenson, "Performance characteristics of polysilicon resonating beam force transducers," in *Integrated Micro-Motion Systems—Micromachining, Control and Applications*, F. Harashima, Ed. 1990, pp. 393–404.

- [17] C. H. Mastrangelo, J. H. Yeh, and R. S. Muller, "Electrical and optical characteristics of vacuum-sealed polysilicon microlamps," *IEEE Trans. Electron Devices*, vol. 39, pp. 1363-1375, 1992.
- [18] L. Lin, C. T.-C. Nguyen, R. T. Howe, and A. P. Pisano, *Microelectromechanical Signal Processors*, U.S. Patent 5 455 547, 1995.
- [19] K. Wang and C. T.-C. Nguyen, "High-order micromechanical electronics filters," in *Proc. IEEE Electro Mechanical Systems (MEMS97)*, pp. 25-30.
- [20] L. Lin, C. T.-C. Nguyen, R. T. Howe, and A. P. Pisano, *Microelectromechanical Signal Processors Fabrication*, U.S. Patent 5 589 082, 1996.
- [21] ———, "Micro electromechanical filters for signal processing," in *Proc. IEEE Micro Electro Mechanical Systems Workshop (MEMS92)*, pp. 226-231.
- [22] X. Zhang and W. C. Tang, "Viscous air damping in laterally driven microresonators," in *IEEE Micro Electro Mechanical Systems Workshop, MEMS94*, pp. 199-204.
- [23] C. T.-C. Nguyen, "Electromechanical characterization of microsensors for circuit applications," Master's thesis, Univ. Calif., Berkeley, 1991.
- [24] L. Lin, "Selective Encapsulations of MEMS: Micro Channels, Needles, Resonators and Electromechanical Filters," Ph.D. dissertation, Univ. Calif., Berkeley, 1993.
- [25] G. T. Mulhern, R. T. Howe, and D. S. Soane, "Supercritical carbon dioxide drying of microstructures," in *Dig. Transducers'93, Int. Conf. Solid-State Sensors and Actuators*, pp. 296-299.
- [26] K. M. McNair, "Microstructure micropackaging," Master's thesis, Univ. Calif., Berkeley, 1991.
- [27] L. A. Field, "Fluid-actuated micromachined rotors and gears," Ph.D. dissertation, Univ. Calif., Berkeley, 1991.
- [28] M. Judy and R. T. Howe, "Polysilicon hollow beam lateral resonators," in *Proc. IEEE Micro Electro Mechanical Systems Workshop (MEMS93)*, pp. 265-271.
- [29] D. J. Monk, P. Krulvitch, R. T. Howe, and G. C. Johnson, "Stress-corrosion cracking and blistering of thin polycrystalline silicon films in hydrofluoric acid," in *Proc. Spring Annu. MRS Conf.*, 1993.
- [30] K. S. Leboutitz, R. T. Howe, and A. P. Pisano, "Permeable polysilicon microshell etch-access windows," in *Dig. Transducers'95, Int. Conf. Solid-State Sensors and Actuators*, vol. 1, pp. 224-227.
- [31] R. I. Pratt, G. C. Johnson, R. T. Howe, and J. C. Chang, "Micromechanical structures for thin film characterization," in *Dig. Transducers'91, Int. Conf. Solid-State Sensors and Actuators*, pp. 205-208.
- [32] H. Guckel, D. W. Burns, H. A. C. Tilmans, D. W. DeRoo, and C. R. Rutigliano, "The mechanical properties of fine-grained polysilicon: The repeatability issue," in *Dig. IEEE Solid-State Sensor and Actuator Workshop*, 1988, pp. 96-99.
- [33] T. I. Kamins and R. S. Muller, *Device Electronics for Integrated Circuits*, 2nd ed. New York: Wiley, 1977.
- [34] C. T.-C. Nguyen and R. T. Howe, "Microresonator frequency control and stabilization using an integrated micro oven," in *Dig. Transducers'93, Int. Conf. Solid-State Sensors and Actuators*, pp. 1040-1043.
- [35] K. Suzuki and H. Tanigawa, "Alternative process for silicon linear micro-actuators," in *Proc. 9th Sensor Symp.*, 1990, pp. 125-128.
- [36] K. Suzuki, "Single-crystal silicon micro-actuators," in *Dig. IEEE Int. Electron Devices Meet.*, 1990, pp. 625-628.
- [37] Y. B. Gianchandani and K. Najafi, "A bulk silicon dissolved wafer process for microelectromechanical devices," *IEEE J. Microelectromech. Syst.*, vol. 1, pp. 77-85, 1992.
- [38] R. S. Payne and D. A. Dinsmore, "Surface micromachined accelerometer: A technology update," in *Proc. SAE Symp.*, 1991, pp. 127-135.
- [39] L. Lin, K. M. McNair, R. T. Howe, and A. P. Pisano, "Vacuum encapsulated lateral microresonators," in *Dig. Transducers'93, Int. Conf. Solid-State Sensors and Actuators*, pp. 270-273.
- [40] W. C. Tang, "Electrostatic comb drive for resonant sensor and actuator applications," Ph.D. dissertation, Univ. Calif., Berkeley, 1990.
- [41] T. M. Bloomstein and D. J. Ehrlich, "Laser deposition and etching of three dimensional microstructures," in *Dig. Transducers'91, Int. Conf. Solid-State Sensors and Actuators*, 1991, pp. 507-511.



**Liwei Lin** received the B.S. degree in power mechanical engineering from National Tsing Hua University, Taiwan, R.O.C., in 1986 and the M.S. and Ph.D. degrees in mechanical engineering from the University of California, Berkeley, in 1991 and 1993, respectively.

From 1993 to 1994, he was with BEI Electronics, Inc. in research and development of microsensors. From 1994 to 1996, he was an Associate Professor at the Institute of Applied Mechanics, National Taiwan University, Taiwan. Since 1996, he has been an Assistant Professor at the Mechanical Engineering and Applied Mechanics Department, University of Michigan, Ann Arbor. He joined the Berkeley Sensor & Actuator Center, an NSF/Industry/University research cooperative center, as a Research Assistant during his graduate study. His research interests are in microelectromechanical systems, including design, modeling, and fabrication of microstructures, microsensors, and microactuators. He holds four U.S. patents in the area of MEMS.



**Roger T. Howe** (S'79-M'84-SM'94-F'96) was born in Sacramento, CA, on April 2, 1957. He received the B.S. degree in physics from Harvey Mudd College, Claremont, CA, in 1979 and the M.S. and Ph.D. degrees in electrical engineering from the University of California, Berkeley, in 1981 and 1984.

He was on the faculty of Carnegie-Mellon University, Pittsburgh, PA, during the 1984-1985 academic year and was an Assistant Professor at the Massachusetts Institute of Technology, Cambridge, from 1985 to 1987. In 1987, he moved to the University of California, Berkeley, where he is now a Professor in the Departments of Electrical Engineering and Computer Sciences and Mechanical Engineering as well as a Director of the Berkeley Sensor & Actuator Center. His research interests include silicon microsensors and microactuators, micromachining processes, and assembly processes.

Dr. Howe served as Cogeneral Chairman of the 1990 IEEE Micro Electro Mechanical Systems Workshop and was General Chairman of the 1996 Solid-State Sensor and Actuator Workshop, Hilton Head, SC.



**Albert P. Pisano** received the Ph.D. degree in the area of high-speed camshaft systems from Columbia University, NY, in 1981.

He is currently the DARPA/ETO MEMS Program Manager and is on administrative leave from his permanent position as Full Professor in the Department of Mechanical Engineering, University of California, Berkeley. He is jointly appointed in the Department of Electrical Engineering and Computer Science and serves as a Codirector of the Berkeley Sensor and Actuator Center and NSF/Industry/University Cooperative Research Center. He has been a Member of Research Staff in the Mechanical Engineering Sciences Area of the Xerox Palo Alto Research Center. He has also held research positions at the General Motors Research Laboratory. In MEMS, he has been active in the design, optimization, and fabrication of resonant structure micromotors, micromechanical grippers, and microtest apparatus for friction and impact measurements.

Dr. Pisano received the NSF Presidential Young Investigation Award for research in optimal mechanical systems design in 1985.